Elastic Instability and Stripe Domains in Liquid Crystalline Elastomers

G. Verwey, M. Warner, E. Terentjev

Elastic Instability and Stripe Domains in Liquid Crystalline Elastomers

G.C. Verwey, M. Warner and E.M. Terentjev (*)

Cavendish Laboratory, University of Cambridge, Madingley Road, Cambridge, CB3 0HE, UK

(Received 23 February 1996, revised 6 May 1996, accepted 30 May 1996)

PACS.61.41.+e – Polymers, elastomers, and plastics
PACS.61.30.Cz – Theory and models of liquid crystal structure
PACS.46.30.Lx – Static buckling and instability

Abstract. — We consider the elastic and orientational response of a uniform nematic elastomer subjected to an extension perpendicular to its director. By allowing a possibility of local shear in the material, we show that the effect of "soft elasticity" leads to a new regime of director reorientation, through a highly non-uniform stripe domain state (in contrast to earlier predictions and observations of a discontinuous uniform director jump). The molecular theory developed here gives predictions on two levels: of the general texture of the stripe state plus the interval of strains in which it occurs, and of topological properties of the director rotation that are very general and depend only on chain anisotropy of elastomer but not on details of the specific material. On the other hand, parameters like the threshold strain for the domain formation depend on the chemical composition and on the model used to describe its effect. We discuss and explain experimental observations of stripe domains both in the perpendicular geometry and when the stretching direction is at an oblique angle to the director, leading to asymmetric stripes and different topology.

1. Introduction

Recently Finkelmann and co-workers [1] have discovered remarkable transitions of a monodomain nematic elastomer under stress to a new, striped state. Our purpose is to explain this transition, using a simple extension of the classical theory of conventional elastomers.

Nematic and high polymer properties are combined in polymer liquid crystals (PLCs). Mesogenic elements (typically rod-like) are incorporated into chains with a residue of flexibility arising from linkages. Such chains can align, the nematic order extending or flattening the chain. Neutron scattering [2] is a suitable tool to monitor the chain shape change. For elastic purposes this is the only important aspect of the nematic order in anisotropic polymer networks. When crosslinked, the chains retain sufficient extensibility that the resulting material is rubbery and can sustain high extensions, and sufficient internal mobility that the average nematic director can easily rotate.

In fact, the director is coupled to the elastic matrix [3] and their relative rotation is penalized by an energy $U = \frac{1}{2}D_1(\boldsymbol{\Omega}-\boldsymbol{\omega})^2$, where $\boldsymbol{\omega}$ is the local rotation of the network and $\boldsymbol{\Omega}$ that of the director. One can view rotations as the antisymmetric part of the elastic deformation tensor $\boldsymbol{\lambda}$.

(*) Author for correspondence (e-mail: emt1000@phy.cam.ac.uk)

This part, λ^A, is trivial in normal solids but of importance in liquid crystal elastomers, where there is an independent internal degree of freedom, the director **n**. Actually the director can be induced to rotate by pure shears, the symmetric part of λ, as well. There is a very rich, non-linear nematic/mechanical (couple stress) elasticity for these new solids.

At a more microscopic level, rubber elasticity is the entropic resistance to imposed changes of shape of chains forming the network. The entropy decreases with the number of available conformations as the chain is extended, and the free energy rises. Since elastomers are driven by their constituent chains' shape, it is not surprising that networks of liquid crystalline polymers can suffer spontaneous shape changes on changing temperature, or respond mechanically when the director is rotated. An illustration is the mechanical "anti-Fredericks" transition [4]. A chain in an aligned nematic rubber will be, say, prolate. Its distribution can be represented by a prolate spheroid, see Figure 1a.

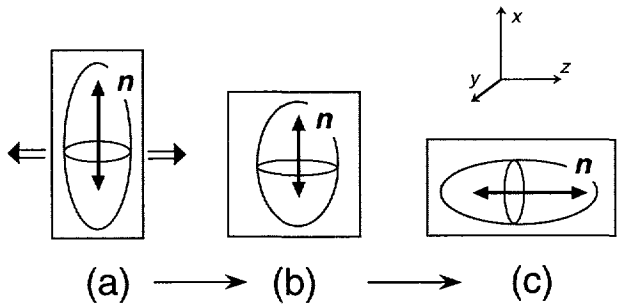

Fig. 1. — Schematic chain conformation in a nematic elastomer under increasing perpendicular extension, leading to eventual re-orientation of the principal axis **n**.

Applying a strain λ in the perpendicular direction distorts chains away from their natural distribution and the free energy rises (Fig. 1b). Eventually, in Figure 1c the elongation is sufficient to accommodate the chains without distortion, if the director rotates by $\pi/2$ to be along λ; an orientational transition then takes place. Ideally the energy in cases (1a) and (1c) is the same, with that of (1b) being higher. Since elastomers deform at constant volume, all deformations are essentially shears and Figure 1 is an extreme example of coupling of **n** to λ^S. Since high deformations are involved, this simple transition lies in the region of non-linear molecular theory. It has been analyzed at length [4, 5] and called anti-Fredericks since the field (mechanical stress) is applied at surfaces, while the director is anchored in the bulk. The director spatial distribution is uniform and the transition is discontinuous, all in contrast to the Fredericks effect in simple nematics [6]. It has been seen by Mitchell *et al.* [7] in an experiment which we shall discuss later.

Mitchell *et al.* [7] clamp the aligned sample in order to impose the transverse extension λ, presumably with the effect that the path between the uniform configurations (1a) and (1c) is not *via* states of simple shear, that is pure shear plus an element of rotation. The samples in the experiment of Finkelmann *et al.* [1], although equally clamped, yield quite different results. Stripe domains, apparent between crossed polars, are formed at a threshold extension λ. Polarized microscopy and X-rays reveal that the director rotates, oppositely in successive stripes, and there is presumably simple shear in each domain, see Figure 2. Gross simple shear has been suppressed due to the clamps on the sample, but it may occur locally, accompanied director rotation within stripes.

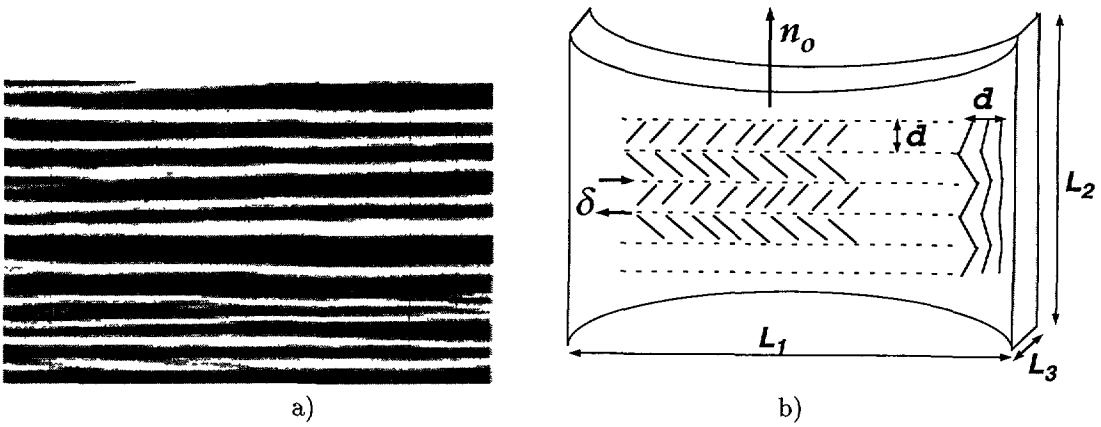

Fig. 2. — The stripe domain texture, as observed by Kundler and Finkelmann [1] (a). The characteristic size of domains is ~ 15 μm; the nematic director rotates in opposite directions in each successive stripe. The scheme of experimental geometry (b), sample dimensions and the decay of local shear near the clamp. This scheme, and the whole theoretical construction, relies on that the clamp region is small and the major portion of the sample undergoes a uniform uniaxial extension.

Actually, banded textures have been seen in the aftermath of shear applied to PLC melts. It has been speculated [8,9] that the relaxation after shear flow involves compression along the director and its accommodation in the form of stripe domains. It is conceivable that for the temporary network of entangled chains in the melt, our model for nematic elastomer stripes may also be applicable.

In elastomers it is apparent from the relative rotation penalty $\frac{1}{2}D(\Omega - \omega)^2$ that if simple shear is permitted, then there is a low energy path between two main conformations (1a) and (1c) of Figure 1 involving rotation of the director. We shall propose that stripe domains are the evidence of such a path being followed, the simple shear of the stripes providing a rotational element to switch the director around at low cost. The final state is that of uniform simple extension. This is essentially the interpretation of Kundler and Finkelmann [1].

In Section 2 we review the neo-classical picture for uniform nematic elastomers, including totally soft modes where mechanical distortions are possible at no free energy cost. We also discuss microscopic effects, in particular fluctuations of chain composition, which prevent the system from achieving total softness. We call this phenomenon "semi-softness". In Section 3 we concentrate on the striped state, calculating the domain wall energy, the end elastic energy in the region near clamps, the stripe width and the threshold strain. Then, in Section 4 we describe the developed stripe domain system and also examine the asymmetric stripes that arise when the principal extension is not exactly perpendicular to the original director. We then conclude by discussing the outstanding problems.

2. Elasticity of Uniform Nematic Elastomers

An anisotropic Gaussian chain is characterized by its mean square dimensions in its principal directions, $\langle R_{\parallel}^2 \rangle = \frac{1}{3}\ell_{\parallel}L$ and $\langle R_{\perp}^2 \rangle = \frac{1}{3}\ell_{\perp}L$, where $\ell_{\parallel}$ and $\ell_{\perp}$ are persistence lengths parallel and perpendicular to the director and L is the contour length of the chain. The lengths $\ell_{\parallel}$, $\ell_{\perp}$, $\ell_{\perp}$ are the eigenvalues of the persistence length tensor describing the spheroid characterizing

the chain shape

$$\boldsymbol{\ell} = \begin{pmatrix} \ell_\parallel & 0 & 0 \\ 0 & \ell_\perp & 0 \\ 0 & 0 & \ell_\perp \end{pmatrix} \quad \rightarrow \ \ell_\perp \left[\boldsymbol{\delta} + (r-1)\,\mathbf{n}\,\mathbf{n}\right] , \tag{1}$$

where $r = \ell_\parallel/\ell_\perp$ is the ratio of principal chain step lengths. The diagonal form of $\boldsymbol{\ell}$ obtains if $\mathbf{n}$ is along a coordinate axis.

The classical (Gaussian) elastic free energy density of conventional rubber generalizes to the neo-classical form for nematic elastomer:

$$f = \frac{1}{2} n_s k_B T \ \mathrm{Tr}\left[\boldsymbol{\ell}_0\, \boldsymbol{\lambda}^T \boldsymbol{\ell}^{-1} \boldsymbol{\lambda}\right] , \tag{2}$$

where $\boldsymbol{\ell}_0$ reflects the chain shape before the deformation $\boldsymbol{\lambda}$ has been imposed, and $\boldsymbol{\ell}$ that of chains in the deformed rubber. n_s is the number of chain strands per unit volume. The initial (before deformation) and current (after) directors $\mathbf{n}_0$ and $\mathbf{n}$ characterize principal directions of $\boldsymbol{\ell}_0$ and $\boldsymbol{\ell}$ as shown in equation (1).

The clamping in Figure 2 is essentially also that of Mitchell *et al.* [7]. The principal extension component of strain, λ_{zz}, is denoted by λ. The other two principal strains are λ_{xx} and $\lambda_{yy} = 1/(\lambda_{xx}\lambda)$, the latter expressing incompressibility. There are no off-diagonal terms since simple shear in the $(x-z)$ plane has been suppressed. The free energies of two states, with $\mathbf{n}$ along $\hat{x}$ (*i.e.* along the initial $\mathbf{n}_0$) and $\mathbf{n}$ along $\hat{z}$, are:

$$f_A = \frac{1}{2} n_s k_B T \left(\lambda^2 + \lambda_{xx}^2 + \frac{1}{\lambda_{xx}^2 \lambda^2}\right) \quad \rightarrow \frac{1}{2} n_s k_B T \left(\lambda^2 + \frac{2}{\lambda}\right) \tag{3}$$

$$f_C = \frac{1}{2} n_s k_B T \left(\frac{\ell_\perp}{\ell_\parallel}\lambda^2 + \frac{\ell_\parallel}{\ell_\perp}\lambda_{xx}^2 + \frac{1}{\lambda_{xx}^2\lambda^2}\right) \rightarrow \frac{1}{2} n_s k_B T \left(\frac{\lambda^2}{\lambda_0^2} + \frac{2\lambda_0}{\lambda}\right) , \tag{4}$$

where the strain λ_0 is shorthand for $r^{1/2} = \sqrt{\ell_\parallel/\ell_\perp}$. At fixed extension λ we can find the optimal transverse contraction λ_{xx}, which equals $\lambda^{-1/2}$ and $r^{-1/4}\lambda^{-1/2}$, in the two cases respectively. The final forms of $f(\lambda)$ have these values of λ_{xx} inserted. Both expressions (3)-(4) are those for a conventional elastomer [10] with natural lengths along the $\hat{z}$ axis of $\lambda = 1$ and $\lambda = \lambda_0$, respectively, see Figure 3a.

The free energies are equal at an extension $\lambda = \lambda_t$ given by $\lambda_t^3 = \lambda_0^2/(1+\lambda_0)$, which is where a discontinuous transition between the initial director orientation $\mathbf{n} = \mathbf{n}_0$ (rotation angle $\theta = 0$) and the final state with $\theta = \pi/2$, $\mathbf{n}$ along λ, would ideally take place. The minima in Figure 3a correspond to the states (1a) and (1c) in Figure 1.

2.1. Soft Deformations. — In general we can allow the director $\mathbf{n}$ to be at an angle with respect to the initial $\mathbf{n}_0$ (and thus the principal frame of $\boldsymbol{\ell}$ is rotated equally from $\boldsymbol{\ell}_0$), and allow a simple shear δ in the relevant $(x-z)$ plane to develop in addition to extensions thus yielding:

$$\boldsymbol{\lambda} \equiv \begin{pmatrix} \lambda_{zz} = \lambda & \delta & 0 \\ 0 & \lambda_{xx} & 0 \\ 0 & 0 & 1/(\lambda_{xx}\lambda) \end{pmatrix} \tag{5}$$

Putting $\boldsymbol{\ell}$ and $\boldsymbol{\lambda}$ into the main free energy density expression (2) gives

$$f = \frac{1}{2} n_s k_B T \left(\lambda^2 + \lambda_{xx}^2 + \frac{1}{\lambda_{xx}\lambda} + r\delta^2 - 2(r-1)\lambda_{xx}\delta \sin\theta\cos\theta \right.$$
$$\left. -(r-1)\left[\frac{1}{r}\lambda^2 - \lambda_{xx}^2 + \delta^2\right]\sin^2\theta\right) \tag{6}$$

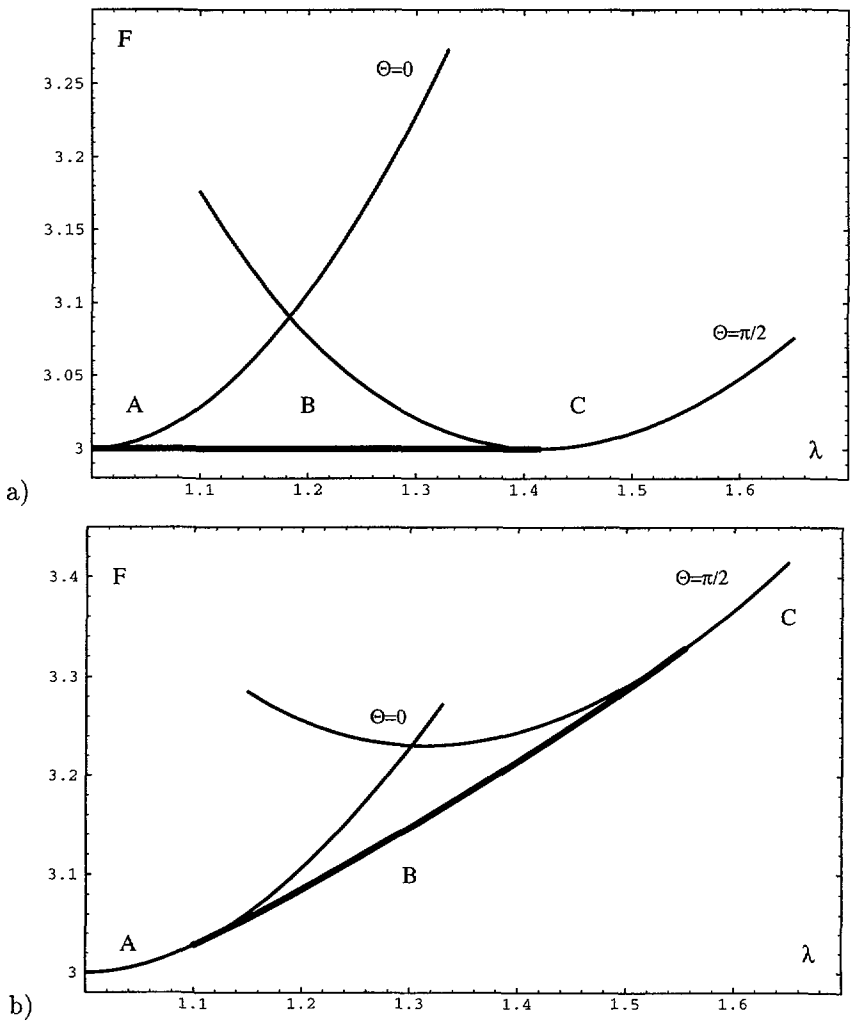

Fig. 3. — Elastic free energy of different configurations in the ideal soft material (a) and in the semi-soft elastomer (b) (see text, Eq. (11) and below). Stripe domains exist in the regime B of transition between the initial state ($\mathbf{n} = \mathbf{n}_0$, $\theta = 0$) and the fully rotated state with $\theta = \pi/2$. The soft (a), or semi-soft (b) trajectory of stripe domains f_B is plotted in bold.

(Suppressing δ and letting $\theta = 0$ or $\pi/2$ one recovers basic Eqs. (3, 4) [4,5].) From (6) it is clear how intimately connected the shear δ and the director rotation θ are. The free energy is evidently lowered by allowing the system to shear and to rotate its director axis accordingly. Equation (6) is somewhat complicated, but minimizing this elastic energy density over δ, θ and λ_{xx} one obtains

$$\lambda_{xx} = \frac{1}{\lambda} \quad \text{(hence} \quad \lambda_{yy} = 1) \,, \tag{7}$$

$$\delta^2 = \frac{1}{r}(\lambda^2 - 1)(r - \lambda^2) \,, \tag{8}$$

$$\sin^2\theta = \frac{r}{r-1}\left(1-\frac{1}{\lambda^2}\right), \tag{9}$$

with the elastic free energy, $f_{\min} = \frac{3}{2}n_s k_B T$. This constant value, equal to the energy of the initial undistorted state ($\lambda = 1$, $\delta = \theta = 0$), does not depend on deformation. It has been called soft elasticity [11]. It can be checked straightforwardly, that putting

$$\boldsymbol{\lambda} = \boldsymbol{\ell}^{1/2}\,\mathcal{R}_\Phi\,\boldsymbol{\ell}_0^{-1/2} \tag{10}$$

into the original free energy (2) (with the matrix $\mathcal{R}_\Phi$ describing an arbitrary rotation) yields a constant $f = \frac{3}{2}n_s k_B T$, *i.e.* this continuous set of non-trivial, volume-conserving strain tensors $\boldsymbol{\lambda}$ leads to *no* rise in the elastic free energy [12]. It is a large class of deformations, characterized by the angles determining the rotation of $\boldsymbol{\ell}(\theta)$ and $\mathcal{R}(\Phi)$. They do not require the application of stress (see also [13]). Following a soft mode, the system can be taken directly from A to C in Figure 3a at no energy cost, provided a suitable shear δ is permitted. The ramifications of soft elasticity in the continuum theory have been discussed at length by Olmsted [12].

Equations (7)-(9) represent a particular case of soft deformation for the elastic energy (6). They show the boundaries of the sheared and rotated state: deformation begins at $\lambda \geq 1$ and ends at extension $\lambda = \sqrt{r} = (\ell_\parallel/\ell_\perp)^{1/2}$ when the rotation of the director is completed, $\theta = \pi/2$.

One can already look forward to an explanation of stripe domains. As extensions $\lambda > 1$ are applied perpendicular to $\mathbf{n}_0$, the transition to the $\theta = \pi/2$ state can proceed *via* the sheared state $\pm\delta$, $\pm\theta$ at little cost. To avoid a macroscopic shear (forbidden by the clamping) the rubber divides into parallel stripes of opposite δ (and θ). There is then an energy cost associated with walls between such opposite domains and the elastic distortion at the end of stripes in order that the clamp constraint is respected. We shall analyze these, and other effects leading to a threshold strain λ_{th} in the next section.

There are however serious problems with this scheme. Figure 3 and equations (7)-(9) show that there is no threshold; stripes should develop immediately $\lambda > 1$. The energy cost of the walls is no help – the creation of a wall (to allow shear in domains on both sides) always lowers the energy from the initial $f_x(\theta = 0)$ toward the line A-C in Figure 3a. The elastic energy contained in the clamp region does lead to a threshold, but it is very small ($\lambda \sim 1 + 10^{-3}$) as we shall discuss in the next section. In experiment [1] the apparent threshold extension is of the order $\lambda \sim 1.1$ and clearly another mechanism for a threshold must be sought. Many candidates suggest themselves, for instance compositional fluctuations, or the effect of using bulky rod-like crosslinks on the second stage of the material synthesis; both act to reduce the apparent softness and thus introduce a threshold. We give one example here to make our discussion concrete. Other mechanisms will have the same qualitative effect, that is to provide a small resistance to all soft deformations in the free energy (6).

2.2. Compositional Fluctuations; Semi-Soft Deformations. — The polymer chains of Mitchell *et al.* are in fact random copolymers ([1]). One type of monomer is intrinsically mesogenic and develops an order parameter, the other is non-nematic and is used as a site for potential crosslinking. Thus the composition of strands between crosslinks randomly varies about the mean composition, the fluctuations about this mean generating fluctuations in the effective step lengths $\ell_\parallel$ and $\ell_\perp$, and thus also in the anisotropy r. Total softness becomes impossible: a soft $\boldsymbol{\lambda}$-trajectory (10) for one polymer strand is not quite what is required for

([1]) Finkelmann *et al.* assemble their networks in such a way that any incompletion or defect in their reactions will effectively yield structural fluctuations. These effects are possibly small in their systems and are dominated by the rodlike character of their crosslinks.

another strand with a slightly different ℓ_0 and ℓ. This destruction of total soft elasticity by compositional fluctuations has been calculated [14] and is evident from equation (6). Averaging the free energy density (6) over different strands, $\langle ... \rangle$, we should replace the anisotropy parameter r by $\langle r \rangle = \langle \ell_\parallel / \ell_\perp \rangle$ wherever it appears. The free energy density averaged over the whole system takes the form

$$\langle f \rangle = f_{\langle r \rangle} + \frac{1}{2} n_s k_B T \left[\langle \frac{1}{r} \rangle - \frac{1}{\langle r \rangle} \right] \lambda^2 \sin^2 \theta \ . \tag{11}$$

The first term, $f_{\langle r \rangle}$, is exactly equation (6) with implemented substitutions $r \to \langle r \rangle$ and $1/r \to 1/\langle r \rangle$, that is unconditionally replacing r with its compositional average. In fact, $\langle 1/r \rangle$ is not exactly equal to $1/\langle r \rangle$, and the corresponding error is corrected by the additional term in (11).

The first part $f_{\langle r \rangle}$ is simple as before and λ_{xx} and δ appear in it exactly as in (6). Thus much of the previous analysis applies. Minimizing with respect to λ_{xx}, δ and θ, we then obtain for the optimal deformation trajectory λ_{xx}, δ and θ:

$$\lambda_{xx} = \frac{\sqrt{\lambda_1}}{\lambda} \ , \qquad \delta_0 = \frac{1}{2} \sin 2\theta_0 \frac{\langle r \rangle - 1}{\langle r \rangle^{1/2}} \frac{\lambda}{\lambda_1} \ , \tag{12}$$

$$\sin^2 \theta_0 = \frac{\langle r \rangle}{\langle r \rangle - 1} \left(1 - \frac{\lambda_1^2}{\lambda^2} \right) \ , \tag{13}$$

where the threshold strain

$$\lambda_1^3 = \frac{1 - 1/\langle r \rangle}{1 - \langle 1/r \rangle} \tag{14}$$

is the final significant strain in the problem and is a measure of the fluctuations (*i.e.* of how $\langle 1/r \rangle$ differs from $1/\langle r \rangle$). This "semi-soft" solution starts at $\lambda = \lambda_1$ where the rotation angle θ and local shear δ grow continuously from zero and λ_{xx} continues to diminish from $1/\sqrt{\lambda_1}$. At the other end of this process, as the main extension $\lambda \to \lambda_1 \sqrt{r}$, the director rotation saturates at $\theta = \pi/2$ and the shear δ returns to zero. These solutions qualitatively resemble the ideally soft situation, described by equations (7)-(9), with the exception that the threshold is now raised above $\lambda = 1$ and that the free energy density is not $\frac{3}{2} n_s k_B T$, but

$$f_B = \frac{1}{2} n_s k_B T \left[\lambda^2 \left(1 - \frac{1}{\lambda_1^3} \right) + \frac{3}{\lambda_1} \right] \tag{15}$$

Both soft and semi-soft cases are characterized by the transverse components of strain $\lambda_{yy} =$ const and $\lambda_{xx} \sim 1/\lambda$, rather than both $\sim 1/\sqrt{\lambda}$ as in any conventional hard regime (see also Sect. 4.2, Eq. (35)).

Figure 3b shows the free energy of this semi-soft trajectory from the initial $\theta = 0$ state at $\lambda = \lambda_1$, to the final one with $\theta = \pi/2$ at $\lambda = \sqrt{r}\lambda_1$. The free energy (15) is tangential to (3) at $\lambda = \lambda_1 \quad (\theta = \delta = 0)$, a fact we shall use in the next section. This free energy of the semi-soft state is also tangential to the one of the final rotated state at $\lambda = \lambda_1 \sqrt{\langle r \rangle} \quad (\theta = \pi/2, \ \delta = 0)$

$$\begin{aligned} f_C &= \frac{1}{2} n_s k_B T \left(\langle \frac{1}{r} \rangle \lambda^2 + \langle r \rangle \lambda_{xx}^2 + \frac{1}{\lambda_{xx}^2 \lambda^2} \right) \ \to \ \frac{1}{2} n_s k_B T \left[\langle \frac{1}{r} \rangle \lambda^2 + \frac{2\sqrt{\langle r \rangle}}{\lambda} \right] \\ &\equiv \frac{1}{2} n_s k_B T \left[\lambda^2 \left(1 - \frac{1}{\lambda_1^3} + \frac{1}{\langle r \rangle \lambda_1^3} \right) + \frac{2\sqrt{\langle r \rangle}}{\lambda} \right] \end{aligned} \tag{16}$$

which is the fluctuation-amended form of (4), with $\lambda_{xx} = \langle r \rangle^{-1/4} \lambda^{-1/2}$. The initial explanation of stripe domains can now be given in terms of the semi-soft elastic response of nematic elastomers. Compositional fluctuations have offered a mechanism for a threshold at finite extension $\lambda_1 > 1$, but there are other mechanisms for the loss of soft elasticity, which will provide a different prefactor in the last ($\sin^2\theta$)-term of (11). Examples are combinations of rigid rod-like crosslink and two-step crosslinking effects. These will, in a similar fashion, lead to a different small threshold strain λ_1, but will leave the qualitative features of the transition unchanged. We, therefore, shall proceed to discuss stripe domains in some detail, in the general terms set down by equations (11)-(15). We shall return to the questions of concrete models for semi-softness and of thermal/mechanical/chemical histories of elastomers in a future paper.

3. The Elastic Instability

We shall first calculate the properties of stripes formed in response to strain imposed perpendicularly to the initial director $\mathbf{n}_0$. The interesting case of oblique extension will be briefly examined in the next section, after the general principles have been established.

It is clear that if local shear deformation is allowed, there exist low energy routes between the initial state of nematic elastomer with $\theta = 0$ and the configuration with $\theta = \pi/2$. Since the global shear deformation of the sample is prohibited by clamping, we propose that such shear and intermediate rotation of $\mathbf{n}$ can exist in bands of alternating sign. Figure 2b shows alternating domains of width d, the displacement associated with the shear δ being indicated in the clamp region. Macroscopically, these displacements are small, but still have to be reconciled with the clamp constraint. We calculate the end energies thus incurred and the energy of nematic and elastic deformations associated with the interface region between the adjacent domains.

3.1. The End Energy. — The amplitude of displacement at the sample ends, with respect to a clamp constraint, Figure 2b, is $\sim d\delta$. This displacement has to decay, thus imposing an additional distortion (extension or compression as required) in a band of elastomer near the clamp. The size of such region, in which elastic strains and the director orientation decay from the optimal semi-soft values of the bulk (12)-(13), is of the order d (stripe width) since the distortion is periodic in the $\hat{x}$ direction with period d. This can be understood, for instance, from the compatibility condition for elastic strains. In the decay region the shear strain $\delta = \lambda_{zx}(x, z)$ and, therefore, must comply with λ_{zz}. $\frac{\partial}{\partial z}\delta = \frac{\partial}{\partial x}\lambda_{zz}$. Clearly, the natural length scale for the $\lambda_{zz}(x)$ variation is the stripe periodicity d and so must be that of the shear decay. Hence the end energy per stripe is $\sim \frac{1}{2}(\mu\delta^2)d^2L_3$. Here μ is the typical (shear) modulus of elastomer and d^2L_3 is volume of the region. We shall denote the parameter $\mu = 3n_s k_B T$ since this is the value of rubber modulus in the isotropic phase and it remains the characteristic energy scale of this problem. There are L_2/d stripes across the sample, whence the total end energy is

$$F_{\text{end}} \approx \frac{1}{2}(\mu\delta^2)L_2L_3d \tag{17}$$

(see Fig. 2b for the sample dimensions, L). This energy decreases as the domain size d gets smaller because the more frequent sign reversal of elastic shear makes it easier to accommodate in the clamp region.

3.2. The Domain Wall Energy. — We now calculate the energy of an isolated wall separating domains with opposite sense of shear and rotation. Experimentally [1] stripes appear

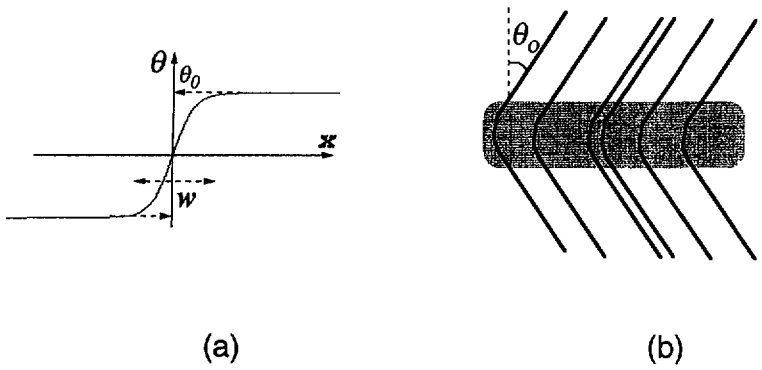

Fig. 4. — The director rotation angle (a) and the scheme of domain interface of the width w. The optimal director angle $\pm\theta_0$ corresponds to the soft (Eq. (9)) or semi-soft (Eq. (13)) solutions.

to have a uniform angle θ_0, the wall between them being very narrow compared with the domain size d. We shall see *post hoc* from the calculation that the assumption about the narrow, solitary wall is justified.

Traversing a wall the director angle $\theta(x)$ varies from θ_0 to $-\theta_0$ *via* $\theta = 0$, see Figure 4a. (We shall exclude for the moment the topologically unrelated possibility of the rotation through $\theta = \pi/2$, or out-of-plane twist within the wall). In this event the energies of states with an intermediate rotation angle $-\theta_0 < \theta < \theta_0$ are required. This means that the system cannot reach its local optimal trajectory, equations (12), (13), and the deformations (at fixed director angle θ) are ([2])

$$\lambda_{xx} = \frac{1}{\sqrt{\lambda}\langle r\rangle^{1/4}}(\langle r\rangle - (\langle r\rangle - 1)\sin^2\theta)^{1/4}\,, \qquad \delta = \frac{(\langle r\rangle - 1)\sin\theta\cos\theta}{\langle r\rangle - (\langle r\rangle - 1)\sin^2\theta} \tag{18}$$

The corresponding free energy, scaled by a factor $\frac{1}{2}n_s k_B T$, takes the form

$$f_\lambda(\theta) \sim \lambda^2 + \frac{2\sqrt{\langle r\rangle}}{\lambda\sqrt{\langle r\rangle - (\langle r\rangle - 1)\sin^2\theta}} - \frac{\langle r\rangle - 1}{\langle r\rangle}\frac{\lambda^2}{\lambda_1^3}\sin^2\theta\,. \tag{19}$$

The wall structure is determined, as usual for interfaces, by the balance between two opposing demands: to traverse the unfavourable region $\theta \sim 0$ as quickly as possible so as to minimize $f_\lambda(\theta)$, and as slowly as possible to minimize the nematic Frank elastic energy by reducing the gradient of $\theta(x)$. The optimal trajectory $\theta(x)$ across the domain wall is determined by minimization of the total energy

$$F \approx L_1 L_3 \int_{-\infty}^{\infty}\left[\frac{1}{2}n_s k_B T f_\lambda(\theta) + \frac{1}{2}K\left(\frac{\mathrm{d}\theta}{\mathrm{d}x}\right)^2\right]\mathrm{d}x\,, \tag{20}$$

where $L_1 L_3$ is the area of a wall. This is a classical problem and yields explicit expressions for the interfacial width w and the wall energy per unit area, γ. For small amplitude bands there

([2]) This form of λ_{xx} and $\delta(\theta)$ is an approximation, neglecting the effect of induced shear λ_{yx} due to the compatibility constraint. Another estimate can be obtained by fixing λ_{xx} and then finding $\delta(\sin\theta)$ alone. The results for wall thickness and energy remain unchanged in this case.

are approximate forms

$$w \approx \sqrt{\frac{K}{\mu}} \left(\frac{\langle r \rangle}{\langle r \rangle - 1} \right)^{1/2} \varepsilon^{-1/2} \tag{21}$$

$$\gamma \approx \frac{1}{3} \sqrt{K\mu} \left(\frac{\langle r \rangle}{\langle r \rangle - 1} \right)^{1/2} \varepsilon^{3/2} \tag{22}$$

where ε is the strain above the threshold, $\lambda = \lambda_1 + \varepsilon$. As usual the energy is proportional to the geometric mean $\sqrt{K\mu}$ of the two competing energy scales and the characteristic width $\xi = (K/\mu)^{1/2}$ sets the scale of w. ξ is associated with the balance of Frank and rubber elasticity in the domain interface and is a microscopic length (for $K \sim 10^{-11}$ N, $\mu \sim 10^5$ J/m^3 we have $\xi \sim 10^{-8}$ m).

The number of domain walls is L_2/d, thus the total energy contained in these walls is

$$F_{\text{wall}} = \gamma \frac{L_1 L_2 L_3}{d} \tag{23}$$

This energy decreases with increasing d because, obviously, one has fewer walls in the system.

3.3. The Domain Size. — The resulting structure of stripes is determined by the balance between the end and the wall energies obtained above. One needs to minimize the total energy of distortions,

$$F(d) = L_1 L_2 L_3 \left(\frac{1}{2} \mu \delta_0^2 \frac{d}{L_1} + \gamma \frac{1}{d} \right) , \tag{24}$$

which gives for the transverse dimension of stripes:

$$d = \sqrt{\frac{2\gamma L_1}{\mu \delta_0^2}} \sim \sqrt{\xi L_1} . \tag{25}$$

The stripe width depends on the geometric mean of ξ and a macroscopic length, the sample dimension along the axis of strain, L_1. The overall energy F_{stripes} of non uniformities in the system is $F_{\text{stripes}} = L_1 L_2 L_3 \sqrt{2\gamma\mu\delta_0^2/L_1}$.

We have seen that the interface energy $\gamma \sim \varepsilon^{3/2}$ and vanishes at the ideal threshold $\lambda = \lambda_1$ of the semi-soft material. The same is true for the optimal magnitude of shear (see Eq. (12)), $\delta_0 \sim \varepsilon^{1/2}$ Therefore, the domain width must vanish at this threshold as well:

$$d \sim 6^{3/4} \sqrt{\xi L_1} \left[\frac{\langle r \rangle}{(\langle r \rangle - 1)^3} \frac{1}{\lambda \lambda_1} \right]^{1/4} \varepsilon^{1/4} \tag{26}$$

Clearly, if the transition into the stripe domain state were to take place exactly at $\lambda = \lambda_1$, as the semi-soft theory predicts, the domain size would be rapidly increasing from zero and we must analyze the transition more accurately.

3.4. The Threshold and Nature of the Transition. — The energy cost of creating stripes must be balanced against the reduction in energy density, $\Delta f = f(\theta = \theta_0) - f(\theta = 0)$, achieved as the system shears to the semi-soft trajectory. As we noted in Section 2, these two branches of energy are tangential to each other at $\lambda = \lambda_1$, that is where $\theta_0 = 0$, and hence this difference $f(\theta = \theta_0) - f(\theta = 0)$ must be quadratic in $\lambda - \lambda_1$, see Figure 3b. In fact,

$$\Delta f = f(\lambda; \theta = \theta_0) - f(\lambda; \theta = 0) = -\frac{1}{2} \mu \frac{\varepsilon^2}{\lambda_1^3} , \tag{27}$$

which is to be balanced against the rise (per unit volume)

$$f_{\text{stripes}} = \frac{F_{\text{stripes}}}{L_1 L_2 L_3} = \sqrt{2\frac{\gamma\mu\delta_0^2}{L_1}} \sim \varepsilon^{5/4} \tag{28}$$

Clearly, at $\varepsilon \ll 1$ the positive energy of stripes (28) is dominant over (27). The energy gain due to the uniform shear and rotation within each domain, expressed by Δf, becomes sufficient to overcome this barrier at the critical deviation

$$\varepsilon_{\text{th}} = 8\left(\frac{\xi}{L_1}\right)^{2/3} \lambda_1^2 \left[\frac{4}{3}\langle r\rangle(\langle r\rangle - 1)\right]^{1/3} \tag{29}$$

This increment over the "ideal" transition strain λ_1, due to the non-uniform distortions in the system, turns out to be very small. For typical values $\xi \sim 10^{-8}$ m, $L_1 \sim 10^{-2}$ m, $\lambda_1 \sim 1$ and the chain anisotropy $r \sim 2$ [1], we obtain $\varepsilon_{\text{th}} \sim 10^{-3}$ Therefore the cost of deforming the ends of stripes in order to conform to the clamp is not sufficient to shift the transition measurably from the underlying threshold λ_1 for semi-soft deformations.

We can now return to equation (26) and estimate the stripe width d at the transition. Because the transition has been slightly delayed, d does not increase continuously from zero. Taking the above estimate for ε_{th} we have $d_{\text{th}} \sim \sqrt{\xi L_1} \sim 10^{-5}$ m. As the imposed deformation λ is increased further beyond $\lambda_1 + \varepsilon_{\text{th}}$ there should be a further increase in d beyond d_{th}, but given the low power $\varepsilon^{1/4}$, this further change will be weak. It is not clear in any event how the stripes can readily alter their width because of the topological problem of removing soliton-like domain walls (see [15] for the analogous situation in stripe domains of a different nature). It is likely that the stripe width remains largely constant as λ is increased.

It is straightforward to estimate small discontinuous jumps of other parameters at ε_{th}, for instance, the director rotation angle within stripes starts at the value

$$\theta_{\text{th}} \approx \pm\left[2\frac{\langle r\rangle}{\langle r\rangle - 1}\frac{\varepsilon_{\text{th}}}{\lambda_1}\right]^{1/2} \sim 3 - 5\,^\circ \tag{30}$$

In summary:
i) The transition takes place at $\lambda \approx \lambda_1$, given by equation (14), with a singular evolution $\theta(\lambda)$ from $\theta = 0$;
ii) Due to end effects the transition is slightly delayed and there is a small jump just beyond λ_1;
iii) The stripe width also does not grow from zero but appears at a finite value, $\sim 10^{-5}$ m, and should change very little thereafter.

4. The State of Stripe Domains

4.1. ANGULAR DEPENDENCE. — As has been discussed in the previous section, the stripe domains are formed in order to comply with the mechanical clamping of the sample, which prevents the net shear deformation and forces the material to break into stripes with shear δ of alternating sign. This argument does not require that the stripes are periodic, but only sets a characteristic length scale d of their average width.

Within stripes the angle of uniform director rotation is given by equation (13), which can be re-written explicitly:

$$\theta_0 = \pm\arcsin\left[\frac{\langle r\rangle}{\langle r\rangle - 1}\left(1 - \frac{\lambda_1^2}{\lambda^2}\right)\right]^{1/2} \tag{31}$$

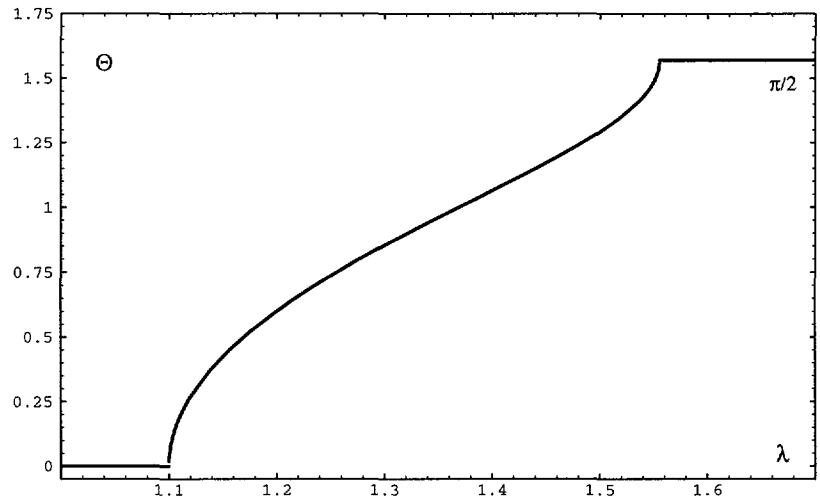

Fig. 5. — Variation of the director rotation angle $\pm\theta(\lambda)$ within stripe domains (regime B between the onset threshold λ_1 and the completion point at $\sqrt{\langle r\rangle}\lambda_1$). Note the singular points at both ends of this regime.

and is plotted in Figure 5 for the values of the mean anisotropy $\langle r\rangle = 2$ and threshold strain $\lambda_1 \sim 1.1$ (see [1]). This expression gives the optimal angle of the director, but we now know that the rotation starts at a threshold (29) slightly higher than λ_1. However, the initial jump in θ_0, equation (30), at $\lambda_1 + \varepsilon_{\rm th}$ is small and, since the dependence $\theta(\lambda)$ is singular with infinite slope at $\lambda = \lambda_1$, it would be hard to distinguish the jump $\theta_{\rm th}$ on top of the underlying "defect-free" behaviour.

Figure 5 also reveals that $\theta(\lambda)$ is singular at the end of the semi-soft regime, $\lambda \to \sqrt{\langle r\rangle}\lambda_1$, $\theta \to \pi/2$. We thus predict in Figure 5 that samples with different compositional fluctuations and thus different λ_1 should have their $\theta(\lambda)$ curves collapse on each other if plotted against λ/λ_1, provided they have similar chain anisotropy $\langle r\rangle$ values.

There remains a question of whether (13) and (31) describe $\theta_0(\lambda)$ correctly in the whole range of deformations, until $\theta_0(\lambda)$ reaches $\pi/2$ at $\lambda = \lambda_1\sqrt{\langle r\rangle}$. If the domain wall remains topologically unchanged, see Figures 4 and 6a, with the plane director bending from θ_0 to $-\theta_0$ through $\theta = 0$, then equation (31) should be the correct dependence for $\theta_0(\lambda)$. This means, however, that the topologically stable wall defect will have to remain between each stripe even in the final fully rotated state (1c) with $\theta_0 = \pm\pi/2$ and zero shear. The effective wall thickness w is very small, as suggested by equation (21), but could perhaps still be visible on the background of totally uniform director field, especially since in crossed polars all would be dark except these "topological fossils". The experiments of Kundler and Finkelmann [1] suggest that some remains of stripe texture can indeed be seen in the final state. The same argument applies to the end zone near the clamp: the director distortion corresponding to the topologically stable bend domain wall cannot easily disappear and the trace of the wall should be seen on top of the uniform background in that region, see Figure 6a.

The alternative route between stripes, Figure 6b, has a different topological nature and there can be no continuous transformation between walls of the types 6a and 6b. As we have asserted above, the system that starts its rotation from the uniform state with $\theta_0 = 0$ will develop bend walls, Figure 6a, which then will remain in the system even after the transition to $\theta_0 = \pi/2$

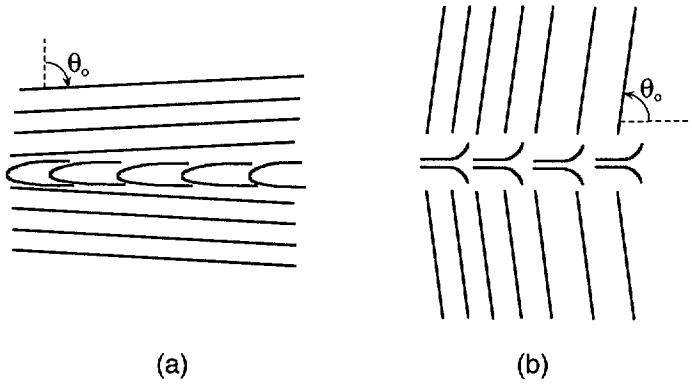

Fig. 6. — Topologically stable wall defects between stripes. The wall of type (a) will remain if the director rotation starts from $\theta_0 = 0$ (*i.e.* $\mathbf{n} = \mathbf{n}_0$) and proceeds towards $\theta_0 = \pi/2$. Type (b) walls would appear if the rotation were instead from the homogeneous state $\theta_0 = \pi/2$. This could be realized by stretching in the isotropic state, then cooling and releasing the strain slowly.

within stripes has taken place. If, however, the stretched state of nematic elastomer with $\theta = \pi/2$ is made completely uniform (for instance, by heating the system into the isotropic state and then cooling back to nematic) the opposite scenario should take place on removing the strain. On decreasing the imposed extension λ the material will seek a route to reach its equilibrium state with $\mathbf{n} = \mathbf{n}_0$ and $\theta = 0$. The semi-soft stripe domain texture is one such route and, clearly, the domain walls of the type 6b will be formed in this case (their energy penalty vanishes completely in the starting configuration with $\theta = \pi/2$, just as we had it for bend walls 6a, equation (22), at their point of formation). For the same topological reasons these new domain walls will have to remain in the system, on the background of the uniform ground state $\theta = 0$ conformation. This interesting speculation could easily be tested by observation.

4.2. STRESS-STRAIN BEHAVIOUR. — The regime $\lambda = \{1, \lambda_1\}$ is elastically "hard" because the branch $f_A(\lambda)$ (see Fig. 3b) is followed. Between λ_1 and $\sqrt{\langle r \rangle}\lambda_1$ semi-soft stripes develop and for $\lambda > \sqrt{\langle r \rangle}\lambda_1$ the material becomes hard again, following $f_C(\lambda)$. The relevant free energies for these regimes are given by equations (3), (15) and finally (16). Therefore, we can calculate the nominal stress $\sigma_i = \mathrm{d}f_i/\mathrm{d}\lambda$ and also the gradient $\mathrm{d}\sigma_i/\mathrm{d}\lambda$, a measure of the modulus at finite extensions. One has for the nominal stresses and moduli in the initial hard, semi-soft and rotated hard regimes:

$$\sigma_A = \frac{1}{3}\mu\lambda\left(1 - \frac{1}{\lambda^3}\right), \qquad \frac{\mathrm{d}\sigma_A}{\mathrm{d}\lambda} = \frac{1}{3}\mu\left(1 + \frac{2}{\lambda^3}\right) \tag{32}$$

$$\sigma_B = \frac{1}{3}\mu\lambda\left(1 - \frac{1}{\lambda_1^3}\right), \qquad \frac{\mathrm{d}\sigma_B}{\mathrm{d}\lambda} = \frac{1}{3}\mu\left(1 - \frac{1}{\lambda_1^3}\right) \tag{33}$$

$$\sigma_C = \frac{1}{3}\mu\lambda\left(1 - \frac{1}{\lambda_1^3} + \frac{1}{\lambda_1^3\langle r \rangle} - \frac{\sqrt{\langle r \rangle}}{\lambda^3}\right), \qquad \frac{\mathrm{d}\sigma_C}{\mathrm{d}\lambda} = \frac{1}{3}\mu\left(\left\langle\frac{1}{r}\right\rangle + \frac{2\sqrt{\langle r \rangle}}{\lambda^3}\right), \tag{34}$$

where the fluctuation parameter $\langle 1/r \rangle$ is determined by the average chain anisotropy $\langle r \rangle$ and the (observable) threshold strain λ_1, equation (14).

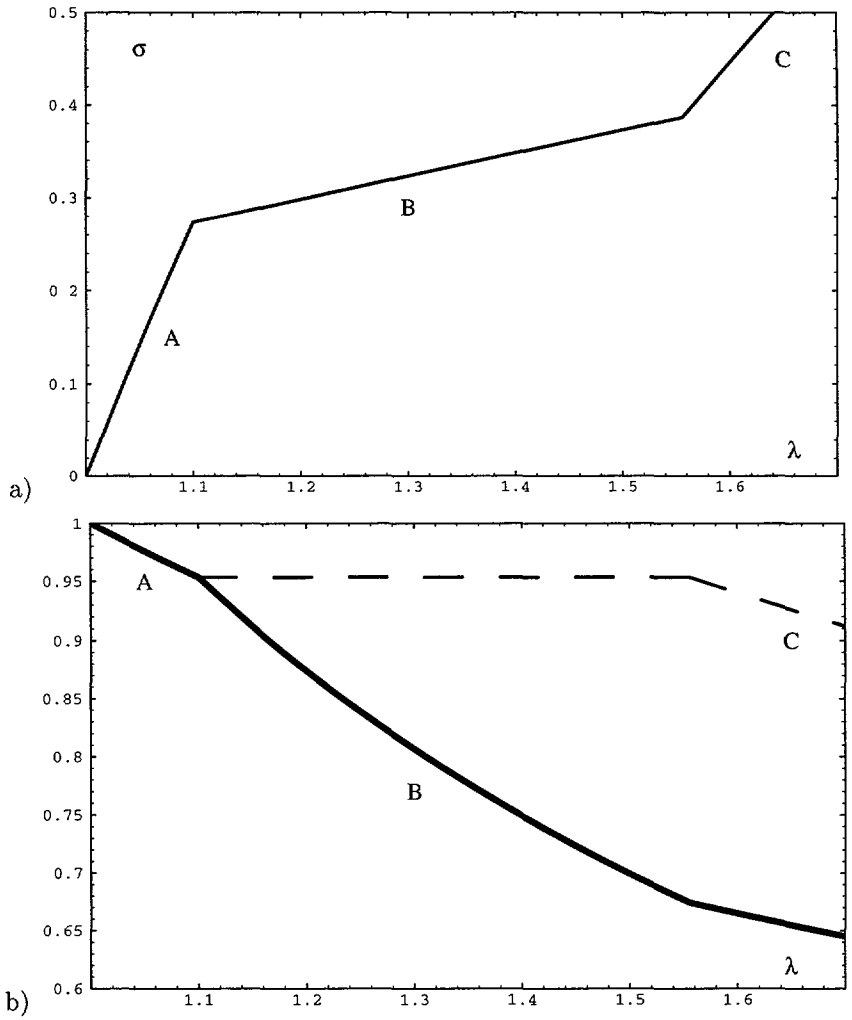

Fig. 7. — (a) Nominal stress σ against strain for hard (A and C) and semi-soft (B) regimes, given by equations (32)-(34). This stress-strain plot is qualitatively the same as that of Küpfer and Finkelmann [16] and thus allows a detailed comparison with experiment. (b) The corresponding transverse strain relaxation, λ_{xx} - solid line and λ_{yy} - dashed line. In the semi-soft regime B $\lambda_{yy} = \text{const}$ and $\lambda_{xx} \sim 1/\lambda$, as for true soft deformations, in contrast to hard regimes A and C where λ_{xx} and $\lambda_{yy} \sim 1/\sqrt{\lambda}$.

These results are schematically presented as a stress-strain curve in Figure 7. There are three regimes, A, B and C on this plot:

• The initial ($\lambda = 1$) slope $\sigma_{\text{A}}(\lambda)$ is the modulus, μ, which sets the scale in equations (32)-(34).

• The important parameter provided by the experiment is the threshold strain $\lambda_1 \approx 1.08$ [1]. Now we can predict the slope of $\sigma_{\text{B}}(\lambda)$ in the stripe regime (33) which turns out to be $\mathrm{d}\sigma_{\text{B}}/\mathrm{d}\lambda \approx \mu/15$. This is a much lower effective modulus: note that its difference from zero is precisely the measure of "semi-softness" – the deviation from the ideal neo-classical theory of nematic elastomers. The deviation is expressed by the correction in equation (11) and shows itself by the presence of a threshold strain λ_1.

• The end of the stripe regime B corresponds to the strain $\sqrt{\langle r\rangle}\lambda_1$, which gives an independent measure of mean anisotropy $\langle r\rangle \approx 2$ [1]. With this data we calculate the slope $\sigma_C(\lambda)$ and the effective modulus in the rotated state C from equation (34), which is $d\sigma_C/d\lambda = 0.44\mu$.

In this analysis we have ignored the contribution to the stress from the work required to create the walls and ends since the shifts in energy they implied were so small (see the discussion in the end of the previous section). Since Küpfer and Finkelmann [16] measured $\sigma(\lambda)$ along with the initial and final strains associated with the stripe interval (λ_1 and $\sqrt{\langle r\rangle}\lambda_1$ in our analysis), direct comparison with experiment is possible (their material and the experimental setup here is almost identical to that of [1]). Figure 5 of [16] shows almost identical qualitative behaviour to the one sketched in Figure 7 here.

Another interesting aspect of deformations in stripe domain state is the transverse contractions λ_{xx} and λ_{yy} (the latter deformation expresses the reduction in the sample thickness L_3, see Fig. 2b). We have seen in the analysis above that in hard elastic regimes $\lambda_{xx} \sim 1/\sqrt{\lambda}$ and $\lambda_{yy} \sim 1/\sqrt{\lambda}$, whereas in the soft or semi-soft regime deformations $\lambda_{xx} \sim 1/\lambda$ and $\lambda_{yy} = \text{const.}$ Thus soft and semi-soft responses are qualitatively identical and quite distinct from the hard one, see Figure 7. There should be a crossover between these two qualitatively different regimes as sharp as the singular behaviour of $\theta(\lambda)$. The explicit results in the three regimes are:

$$\begin{aligned} &\mathsf{A}: && \lambda_{xx} = \lambda_{yy} = \frac{1}{\sqrt{\lambda}} \\ &\mathsf{B}: && \lambda_{xx} = \frac{\sqrt{\lambda_1}}{\lambda}\ ; \qquad \lambda_{yy} = \frac{1}{\sqrt{\lambda_1}} \\ &\mathsf{C}: && \lambda_{xx} = \frac{1}{\langle r\rangle^{1/4}}\frac{1}{\sqrt{\lambda}}\ ; \qquad \lambda_{yy} = \frac{\langle r\rangle^{1/4}}{\sqrt{\lambda}} \end{aligned} \tag{35}$$

Although λ_{yy} may be difficult to measure for a thin strip, λ_{xx} should be straightforwardly accessible and, at a given imposed extension λ, λ_{yy} is derivable by the volume conservation condition.

4.3. Experiments with Strain Perpendicular to $\mathbf{n}_0$. — Mitchell *et al.* [7] performed experiments on monodomain nematic elastomers aligned and then crosslinked in a magnetic field. Finkelmann *et al.* [1, 16] used the two-step crosslinking method when the sample is stretched after the first weak crosslinking reaction to reach a monodomain state, and then crosslinked for the second time. Both groups performed wide angle X-ray scattering (WAXS) to determine the nematic order parameter Q and the director orientation θ. Mitchell *et al.* saw a substantial jump in $\theta(\lambda)$ at a threshold and that the magnitude of the order parameter collapsed at the transition and then recovered. This was at about 70 K below the nematic-isotropic transition. Finkelmann *et al.*, on the other hand, saw the WAXS pattern break into two equivalent but counter-rotated parts ($\pm\theta_0$) with no measurable decline in the order parameter seen in each part, even though these experiments were performed relatively close to the N-I transition. Analysis by crossed polars then confirmed that the two sets of WAXS peaks correspond to the separate $\pm\theta_0$ stripes. The other main difference between the two experiments was that Finkelmann's polymers were of a much higher anisotropy: Küpfer and Finkelmann [16], studying the same material as in [1], measured the spontaneous distortion to be $L/L_0 \sim 1.4$ leading to $r = \ell_\parallel/\ell_\perp \sim 2.5$. Mitchell's polymers [7], an equivalent small temperature below the N-I transition, had a $L/L_0 \sim 1.05$, giving $r \sim 1.16$ (unfortunately the data corresponding to the temperature of their mechanical experiment were not given).

In the analysis of this paper we have assumed that the nematic order is rigid, that is its magnitude Q is unchanged by strains and only its direction responds by rotation. This is

discussed at length in [5] and is justified by comparing elastic and nematic effects in elastomers. Since the elastic energies are of the scale k_BT per chain strand and the nematic energy is per monomer, it is a reasonable assumption, confirmed by Finkelmann's observation of constant values of Q. It is accordingly rather surprising to find in the other case [7], where the nematic order should be even more rigid, that a mechanical transition causes it to collapse. Perhaps the lower intrinsic chain anisotropy is responsible for this effect?

In earlier work [4, 5] Mitchell's results were explained by invoking only uniform states with a transition between states $\theta = 0$ and $\theta = \pi/2$ at either λ_t or at the point of the total stability loss $\lambda = (\ell_\parallel/\ell_\perp)^{1/3}$ in Figure 3a. The present paper, by looking at a more complicated non-uniform state including shear deformations, has showed that there is another, low-energy trajectory for this transition *via* a stripe domain state. This invites the question, why was there not a transition to a striped state, which should mediate the transition between the initial and the final states (1a) and (1c)? It is difficult to answer this question without more data on the intermediate states, for instance WAXS at extension just above the threshold, and measurement of spontaneous chain anisotropy at the experiment temperature.

Finkelmann's data are qualitatively explained by the model we have presented, but the question of detailed modeling the semi-soft threshold strain λ_1, equation (14), remains. Here it has been essentially treated as a phenomenological parameter, simply describing the deviation of a real monodomain nematic elastomer from an ideal soft elasticity regime (see Eq. (11)). Several molecular mechanisms for this departure are possible and, probably, all contribute their part to the prefactor of the addition $\sim \sin^2\theta$ to the neo-classical free energy (2). Throughout this paper we have implicitly adopted just one such model, namely the concept of chain compositional fluctuations [14], leading to the difference between average values $\langle 1/r\rangle - 1/\langle r\rangle$. A simple perturbative analysis [14], within the freely-jointed rod model, yields a rather small value of λ_1. Persistent chains give much higher value for the effect of compositional fluctuations, and we shall return to explicit calculation of this threshold in a future work. There is also the question of the dependence of this threshold strain on the crosslinking density, $\lambda_1(n_s)$. Compositional fluctuations certainly depend on n_s, as does the effect of bulky rod-like crosslinks, for example. Before adopting a definite view on which molecular mechanism dominates the weak, semi-soft elasticity (11) it is necessary to have more data from the experiment. For instance, Finkelmann *et al.* [1], reporting about their sample preparation procedure, indicate that several experimental conditions were varying with n_s, which may cloud the interpretation of the threshold dependence.

4.4. Transition under Oblique Strain. — We briefly consider the situation when the extension is imposed at an oblique angle to the initial director $\mathbf{n}_0$. The free energy density now contains a pre-tilt of the director, $\theta = \alpha$. However, the concept of near-soft deformations as a low energy route for director re-orientation remains valid. For simplicity, we present the result for the ideal "soft" case, which bears no qualitative difference to the real system except that the threshold is offset by λ_1. The direct minimization gives the optimal director rotation angle

$$\sin^2\theta_0 = \frac{1}{\lambda(r-1)}\left[r(\lambda^2-1) + (r-1)\sin^2\alpha\right] \tag{36}$$

and the two modes of shear deformation within each domain are

$$\delta_\pm = -\frac{\lambda^2(r-1)\sin\alpha\cos\alpha \pm \sqrt{r(\lambda^2-1)+(r-1)\sin^2\alpha}\sqrt{r-\lambda^2-(r-1)\sin^2\alpha}}{\lambda[r-(r-1)\sin^2\alpha]} \tag{37}$$

The "positive" domain, δ_+, in which the existing director pre-tilt α is in the same direction, can start its shear deformation continuously. However, in order to form "negative" stripes with

the shear of opposite sense, it is necessary to overcome a barrier - stripes with $-\theta_0$ must jump to that state from the initial orientation. This discontinuous jump in δ_- at the transitions takes the form:

$$\Delta\delta = -\frac{2(r-1)\sin 2\alpha}{r+1+(r-1)\cos 2\alpha} \tag{38}$$

In order to comply with the clamp constraint the domains with such a different magnitude of shear must now have different width, given by the relation

$$d_+\delta_+ = d_-\delta_- \ . \tag{39}$$

Therefore, one should expect the different intensity of scattering from the two sets of domains, determined by their different volume, the ratio of these intensities given by $I_-/I_+ = d_-/d_+$.

5. Conclusions

To summarize, we have described a new non-uniform regime of deformation and re-orientation of monodomain nematic elastomers in an interval of extensions determined by the mean chain anisotropy in the material. This transitional regime is remarkable in that in spite of the system being mechanically constrained, it is able to find a trajectory that is essentially soft. It is the first unambiguous experimental evidence for soft deformations. The texture of this non-uniform deformation is determined by mechanical constraints on the sample (to avoid a macroscopic shear) and has a form of irregular stripe domains of a mean characteristic size d, given by equation (26). Realistic elastomers would have various molecular reasons to be what we call semi-soft, with small deviations from the neo-classical nematic rubber elasticity. In each case the transition would start at a small threshold strain.

The results of this paper form two distinctive groups. The first group gives a set of universal predictions about the transition:

(1) The "window" of extensions, in which the transition is taking place and stripe domains form, is between a small threshold strain λ_1 and the complete re-orientation at $\sqrt{\langle r\rangle}\lambda_1$, with $\langle r\rangle$ the mean chain anisotropy.

(2) The director rotation angle $\theta(\lambda)$ has a characteristic dependence with singularities at the threshold and at the end-point of the stripe regime, equation (31) and Figure 5. There is an associated local shear deformation of opposite sense in each domain.

(3) Due to the defect walls between the domains the real transition is further offset by a very small increment $\varepsilon_{\rm th}$, equation (29). However, due to the singular behaviour of $d(\lambda)$ and $\theta(\lambda)$ near this point, the domains form with a finite spacing $d \sim 10^{-5}$ m, which then changes very little with deformation, $d \sim \varepsilon^{1/4}$

(4) There are three elastic regimes, a hard one before the threshold λ_1, when no rotation of the director takes place and the rubber responds to deformation with a normal transverse modulus μ; a semi-soft deformation of stripe domains, when the director rotates in two opposite directions the apparent modulus is at least an order of magnitude lower; a fully rotated hard regime, when the director is aligned along the stress axis and the effective elastic modulus is only slightly lower than in the initial regime. The corresponding stress-strain relation is sketched in Figure 7.

The other group of results is related to the value of the transition threshold λ_1. This parameter is totally determined by fine details of the material preparation and should be very different in different systems. It is the measure of deviation of a specific sample from neo-classical nematic rubber elasticity, equation (2). There are several molecular mechanisms for such a deviation, which we have discussed in the text and which will be a subject of another

publication. Here we considered one of such mechanisms, based on the effect of compositional fluctuations making different chains in the system to have different values of anisotropy $r = \ell_{\parallel}/\ell_{\perp}$. Within this model the threshold strain λ_1 is given by equation (14), in which the average $\langle 1/r \rangle$ can be regarded as a phenomenological parameter, slightly different from $1/\langle r \rangle$. Intimately related to the fluctuation parameter λ_1 is the apparent modulus in the stripe regime B, equation (33), which is only different from zero in a semi-soft system.

We believe that this analysis, combined with the experimental findings, gives a new insight to the physics of liquid crystalline elastomers, allowing a better understanding of these remarkable materials.

Acknowledgments

We are much indebted to H. Finkelmann and I. Kundler for bringing their stripe domains to our attention, and for many useful discussions and suggestions; EMT and MW acknowledge their hospitality on visits to Freiburg. This research has been supported by EPSRC.

References

[1] Kundler I. and Finkelmann H., *Macromol. Chem. - Rapid Comm.* **16** (1995) 679.
[2] d'Allest J.F., Sixou P., Blumstein A., Blumstein R.B., Teixeira J. and Noirez L., *Mol. Cryst. Liq. Cryst.* **155** (1989) 581.
[3] de Gennes P.G., in Liquid Crystals of One and Two-Dimensional Order, W. Helfrich and G. Heppke Eds. (Springer, Berlin, 1980).
[4] Bladon P., Terentjev E.M. and Warner M., *Phys. Rev. E* **47** (1993) R3838.
[5] Bladon P., Terentjev E.M. and Warner M., *J. Phys. II France* **4** (1994) 75.
[6] de Gennes P.G. and Prost J., The Physics of Liquid Crystals (Clarendon, Oxford, 1993).
[7] Mitchell G.R., Davis F. and Guo W., *Phys. Rev. Lett.* **71** (1993) 2947.
[8] Yan N.X. and Labes M.M., *Macromolecules* **27** (1994) 7843.
[9] Ernst B. and Navard P., *Macromolecules* **22** (1989) 1419.
[10] Treloar L.R.G., The Physics of Rubber Elasticity, 3rd ed. (Clarendon Press, Oxford, 1975).
[11] Warner M., Bladon P. and Terentjev E.M., *J. Phys. II France* **4** (1994) 91.
[12] Olmsted P.D., *J. Phys. II France* **4** (1994) 2215.
[13] Golubovic L. and Lubensky T.C., *Phys. Rev. Lett.* **63** (1989) 1082.
[14] Verwey G. and Warner M., *Macromolecules* **28** (1995) 4303.
[15] Terentjev E.M. and Pikin S.A., *Sov. Phys. JETP* **56** (1982) 587.
[16] Küpfer J. and Finkelmann H., *Makromol. Chem. - Rapid Comm.* **12** (1991) 717.